Development of Reference Specimens for Laboratory Testing

PUBLICATION NO. FHWA-HRT-23-068

MAY 2024

U.S. Department of Transportation
Federal Highway Administration

Research, Development, and Technology
Turner-Fairbank Highway Research Center
6300 Georgetown Pike
McLean, VA 22101-2296

FOREWORD

This report summarizes the results of a study that developed new procedures to fabricate reference specimens for reinforced concrete with defects, including surface cracks, delamination, honeycombing, and reinforcement corrosion. Reference specimens can be used for nondestructive evaluation (NDE) validation purposes for a given test problem and also for qualification/certification of NDE service providers. These reference specimens can also provide valuable research data to help researchers further understand and improve state-of-the-art NDE technologies.

The intended audience for this report is researchers and bridge engineers from Federal, State, and local transportation departments and parties engaged in bridge-related research.

Jean A. Nehme, PhD, PE
Director, Office of Infrastructure
Research and Development

TECHNICAL REPORT DOCUMENTATION PAGE

1. Report No. FHWA-HRT-23-068	2. Government Accession No.	3. Recipient's Catalog No.
4. Title and Subtitle Development of Reference Specimens for Laboratory Testing		5. Report Date May 2024
		6. Performing Organization Code
7. Author(s) Ernst Niederleithinger, Christian Köpp, Juri Timofeev, Hoda Azari (ORCID: 0000-0002-7340-0035), and Simon Shams (ORCID: 0000-0001-6503-1965)		8. Performing Organization Report No.
9. Performing Organization Name and Address Bundesanstalt für Materialforschung und -prüfung, Inc. (BAM) Unter den Eichen 87, 12205 Berlin, Germany		10. Work Unit No.
		11. Contract or Grant No. DTHF61-D-14-00011
12. Sponsoring Agency Name and Address Office of Infrastructure Research and Development Federal Highway Administration 6300 Georgetown Pike McLean, VA 22101		13. Type of Report and Period Covered Final Report; October 2016–April 2024
		14. Sponsoring Agency Code HRDI-20

15. Supplementary Notes
The contracting officer's representative was Hoda Azari (HRDI-20; ORCID: 0000-0002-7340-0035).

16. Abstract
Engineers and bridge owners have widely used nondestructive evaluation (NDE) methods for the assessment and inspection of reinforced concrete structures. The creation of reference specimens featuring structural defects commonly encountered in the field is crucial for enhancing understanding of NDE technologies and certifying NDE service providers. This report presents the findings of a study aimed at establishing novel procedures for producing reference specimens for reinforced concrete structures that replicate common defects, such as surface cracks, delamination, internal honeycombing, and reinforcement corrosion-induced flaws. These procedures closely mimic the structural deficiencies observed in real-world structures. The report documents the efforts of two distinct research laboratories for both method development and validation, referred to as Research Laboratory A and B throughout this report. Research Laboratory A developed procedures to fabricate reference specimens representing common issues in concrete structures. Research Laboratory B implemented these procedures to create the reference specimens and validated the fabrication techniques established by Research Laboratory A. The results of this study lay a foundation for research laboratories to adopt standardized procedures for fabricating reference specimens. These specimens serve as essential tools for evaluating the efficacy of NDE technologies.

17. Key Words	18. Distribution Statement
Reinforced concrete, nondestructive evaluation, reference specimens	No restrictions. This document is available to the public through the National Technical Information Service, Springfield, VA 22161. http://www.ntis.gov

19. Security Classif.(of this report)	20. Security Classif.(of this page)	21. No. of Pages	22. Price
Unclassified	Unclassified	47	N/A

SI* (MODERN METRIC) CONVERSION FACTORS

APPROXIMATE CONVERSIONS TO SI UNITS

Symbol	When You Know	Multiply By	To Find	Symbol
		LENGTH		
in	inches	25.4	millimeters	mm
ft	feet	0.305	meters	m
yd	yards	0.914	meters	m
mi	miles	1.61	kilometers	km
		AREA		
in^2	square inches	645.2	square millimeters	mm^2
ft^2	square feet	0.093	square meters	m^2
yd^2	square yard	0.836	square meters	m^2
ac	acres	0.405	hectares	ha
mi^2	square miles	2.59	square kilometers	km^2
		VOLUME		
fl oz	fluid ounces	29.57	milliliters	mL
gal	gallons	3.785	liters	L
ft^3	cubic feet	0.028	cubic meters	m^3
yd^3	cubic yards	0.765	cubic meters	m^3
	NOTE: volumes greater than 1,000 L shall be shown in m^3			
		MASS		
oz	ounces	28.35	grams	g
lb	pounds	0.454	kilograms	kg
T	short tons (2,000 lb)	0.907	megagrams (or "metric ton")	Mg (or "t")
		TEMPERATURE (exact degrees)		
°F	Fahrenheit	5 (F-32)/9 or (F-32)/1.8	Celsius	°C
		ILLUMINATION		
fc	foot-candles	10.76	lux	lx
fl	foot-Lamberts	3.426	$candela/m^2$	cd/m^2
		FORCE and PRESSURE or STRESS		
lbf	poundforce	4.45	newtons	N
lbf/in^2	poundforce per square inch	6.89	kilopascals	kPa

APPROXIMATE CONVERSIONS FROM SI UNITS

Symbol	When You Know	Multiply By	To Find	Symbol
		LENGTH		
mm	millimeters	0.039	inches	in
m	meters	3.28	feet	ft
m	meters	1.09	yards	yd
km	kilometers	0.621	miles	mi
		AREA		
mm^2	square millimeters	0.0016	square inches	in^2
m^2	square meters	10.764	square feet	ft^2
m^2	square meters	1.195	square yards	yd^2
ha	hectares	2.47	acres	ac
km^2	square kilometers	0.386	square miles	mi^2
		VOLUME		
mL	milliliters	0.034	fluid ounces	fl oz
L	liters	0.264	gallons	gal
m^3	cubic meters	35.314	cubic feet	ft^3
m^3	cubic meters	1.307	cubic yards	yd^3
		MASS		
g	grams	0.035	ounces	oz
kg	kilograms	2.202	pounds	lb
Mg (or "t")	megagrams (or "metric ton")	1.103	short tons (2,000 lb)	T
		TEMPERATURE (exact degrees)		
°C	Celsius	1.8C+32	Fahrenheit	°F
		ILLUMINATION		
lx	lux	0.0929	foot-candles	fc
cd/m^2	candela/m2	0.2919	foot-Lamberts	fl
		FORCE and PRESSURE or STRESS		
N	newtons	2.225	poundforce	lbf
kPa	kilopascals	0.145	poundforce per square inch	lbf/in^2

*SI is the symbol for International System of Units. Appropriate rounding should be made to comply with Section 4 of ASTM E380. (Revised March 2003)

TABLE OF CONTENTS

LIST OF FIGURES

LIST OF TABLES

LIST OF ABBREVIATIONS

FHWA	Federal Highway Administration
GPR	ground-penetrating radar
NDE	nondestructive evaluation
PVC	polyvinyl chloride
SAFT	synthetic aperture focusing technique
UT	ultrasonic tomography

CHAPTER 1. INTRODUCTION

Nondestructive evaluation (NDE) methods for assessing and inspecting reinforced concrete infrastructure have been successfully applied throughout the last decade. However, the confidence and consistency of NDE measurements must be established by developing reference specimens. The value of concrete reference specimens relies on how closely the artificial defects resemble defects in real-world structures. For instance, introducing plastic sheets between reinforcement layers in a specimen cannot correctly represent realistic delamination. Furthermore, real delamination and external objects, such as plastic sheets, differ in material properties, causing discrepancies in NDE results. Creating standard reference specimens with realistic defects is crucial for training and certification programs and for comparing, interpreting, and fusing the results of NDE methods. This study establishes procedures to develop reference specimens with four types of structural defects: cracks, delamination, honeycombing, and reinforcement corrosion.

Defects in concrete specimens should be reproducible in any laboratory to properly compare different NDE methods. The range of variable parameters in constructing reference specimens, such as concrete properties and steel reinforcement sizes, was investigated in this study. The outcome of this investigation will lay the groundwork for quantitative NDE practices and standardizations. Additionally, through the use of reference specimens, NDE methods can follow guidelines that consider application limits, the proper selection of devices, and the use of optimal device settings.

The study enlisted the efforts of two distinct research laboratories for both procedure development and validation, referred to as Research Laboratory A and Research Laboratory B throughout this report. Research Laboratory A developed procedures to fabricate reference specimens. Research Laboratory B evaluated those procedures to ensure the reproducibility of reference specimens at a different research organization.

Chapter 2 presents a comprehensive literature review of existing fabrication methods for the four types of structural defects found in concrete structures, namely cracks, delamination, honeycombing, and reinforcement corrosion.

Chapter 3 outlines the methodology employed by Research Laboratory A for fabricating reference specimens with cracks and includes validation results from Research Laboratory B.

Chapter 4 details the fabrication method for reference specimens with delamination developed by Research Laboratory A and includes validation results from Research Laboratory B.

Chapter 5 describes the methodology used by Research Laboratory A to create reference specimens with honeycombing and provides validation results from Research Laboratory B.

Chapter 6 explains the methodology employed by Research Laboratory A for fabricating reference specimens with reinforcement corrosion and includes validation results from Research Laboratory B.

Chapter 7 offers a summary of the study's findings and their significance.

CHAPTER 2. LITERATURE REVIEW

This study focused on four types of structural defects commonly observed in concrete structures: cracks, delamination, honeycombing, and reinforcement corrosion. This chapter documents the research team's literature review of the existing methods of artificially simulating these four types of structural defects in fabricating concrete specimens and related studies.

CRACKS

Artificially creating cracks in concrete specimens is mainly documented in laboratory studies of concrete structures. The methods developed for generating cracks depend on the research objectives and the type of testing being conducted.

One prominent approach is to use notches to represent cracks (Tran and Roesler 2022). Notches can be skillfully introduced into concrete specimens via saw cutting. In this method, a specialized concrete saw equipped with a diamond blade is employed to cut the concrete surface. This approach enables the creation of cracks with controllable depths and lengths but may introduce a cutting surface that is larger than cracks.

Another frequently employed approach is to insert external objects such as plastic, rubber, or metal into fresh concrete before the curing process, embedding the objects. Upon removal of these objects, this method generates distinctive voids that can evolve into cracks as the concrete undergoes the curing process. As a notable example, Torkornoo et al. (2018) used shims to create cracks of varying widths in concrete structures.

A third approach is to apply controlled mechanical loading to generate cracks in concrete structures. A practical application of this method involves the generation of natural cracks on prisms using a three-point, controlled bending technique (Bogas, Ahmed, and Diniz 2021).

DELAMINATION

Delamination encompasses the separation of layers or the detachment of concrete interfaces with reinforcements. A common method involves inserting plastic, rubber, or metal into fresh concrete, much like the approach used in generating artificial cracks. These inserts are strategically positioned to simulate delamination in the concrete structure. As the concrete cures and hardens, the removal of these inserts creates voids that replicate the characteristics of delamination (Kee and Gucunski 2016; Oh et al. 2013; Sansalone and Carino 1989; Zhu and Popovics 2007).

HONEYCOMBING

The creation of artificial honeycombing in concrete specimens for laboratory assessments involves simulating the presence of concentrated voids or hollow areas within the concrete mix during the curing process. This simulation is accomplished by intentionally diminishing the compaction efforts during the concrete casting process. This process typically entails using vibration or compaction levels less than those levels conventionally recommended for standard concrete placement practices. Consequently, this deliberate approach leads to inadequate filling

of air voids and incomplete consolidation, thereby giving rise to the characteristic honeycombing phenomenon.

Additionally, the choice of aggregates within the concrete mix plays a pivotal role in the occurrence of honeycombing. Specifically, the inclusion of poorly graded or gap-graded aggregates can result in voids and honeycombing. These voids often manifest between the larger and smaller aggregate particles, further contributing to the formation of honeycombing. Shibin et al. (2018) employed an innovative technique involving a bag of loose aggregates covered by a thin layer of concrete in the concrete form. This approach effectively replicated concrete mixtures with a deficiency in structural integrity, facilitating the study of honeycombing in laboratory assessments. It is also worth noting that various types of artificial honeycombs can be introduced into concrete specimens. These artificial honeycombs include single aggregates affixed using a cement paste along a rebar and foam-incorporated aggregates (Stefan et al. 2018).

REINFORCEMENT CORROSION

Researchers have devised two primary approaches for introducing corrosion to concrete specimens. One approach is to embed precorroded rebar within the concrete during the casting process. This precorroded rebar serves as a source of corrosion within the concrete structure. Hassan and Yazdani (2016) proposed a method to provide corroded rebars by applying direct current to intact steel rebar submerged in a 5-percent saltwater solution.

Another approach is to employ an accelerated corrosion setup as the corrosive environment in a controlled manner. Zhang et al. (2016) used this approach to elevate the chloride content in the environment surrounding the rebar within the concrete specimen. The corrosion level and length are managed by controlling the current applied to induce corrosion, following the principles outlined in Faraday's law. Additionally, the size of the region infiltrated by the electrolyte is carefully regulated to achieve the desired outcomes.

REMARKS

The deliberate creation of structural defects in concrete specimens is a versatile practice, with methods tailored to the specific research goals and testing requirements. This study focuses on developing a new method for generating cracks and delamination. The proposed method aims to generate both surface and internal cracks without surface cutting, inserting external nonconcrete objects, or applying physical loadings. The study also validates common practices in producing internal honeycombing and reinforcement corrosion in concrete.

CHAPTER 3. CRACKS

BACKGROUND

Creating artificial cracks is a challenging task. This study developed an approach for fabricating concrete specimens with surface and internal cracks without embedding nonconcrete objects. The method necessitates creating a row of blind holes on the surface of the concrete specimen. Filling the blind holes with expandable material can generate surface and internal cracks. This study used a swelling clay material that could expand and generate internal cracks within 24 hr.

Figure 1 illustrates the proposed method for creating surface and internal cracks in concrete specimens. The key design philosophy is to find the appropriate diameter, spacing, and drilling depth of the blind holes so that the generated surface and internal cracks are desirable and reproducible. The desired surface cracks will be large enough to be visible on the specimen surface, and the internal cracks will propagate in the direction of the thickness of the specimen. The shape of the internal cracks will be as planar as possible, and their depths will be predictable.

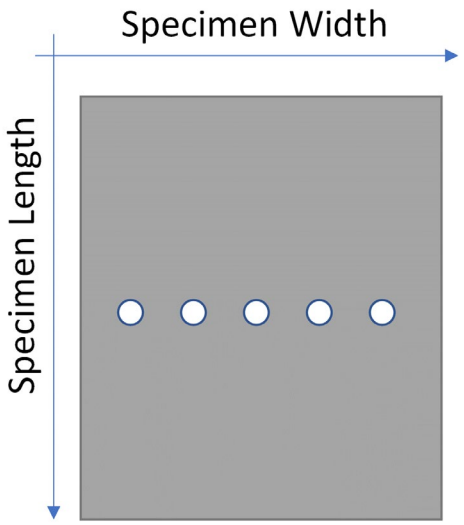

Source: Federal Highway Administration (FHWA).

A. Reference specimen with row of boreholes.

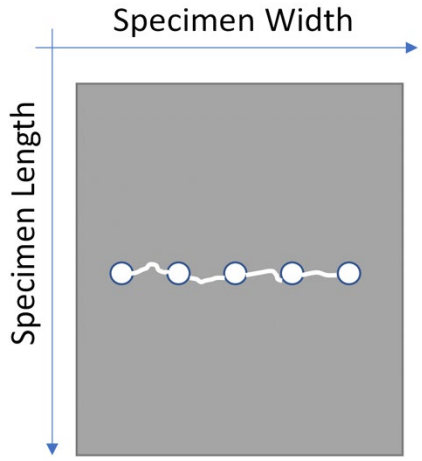

Source: FHWA.

B. Surface cracks that developed between boreholes.

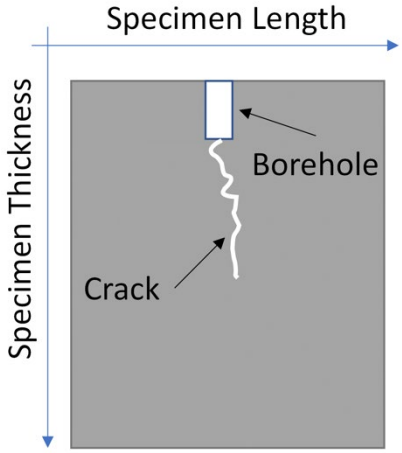

Source: FHWA.

C. Internal cracking that developed under a borehole.

Figure 1. Diagram. Proposed method for creating internal cracks in concrete specimens.

This study fabricated three specimens to determine the optimum design parameters for the blind holes. With improperly designed blind holes, the specimen can be entirely split (figure 2). The design parameters were first developed by Research Laboratory A and then repeated and validated by Research Laboratory B.

Source: FHWA.

Figure 2. Photo. Total split of the specimen due to improper borehole design.

IMPLEMENTATION BY RESEARCH LABORATORY A

Research Laboratory A used European standard EN 206-1:2000/A2:2005—*Concrete—Part 1: Specification Performance, Production and Conformity* for specimen design and fabrication (National Standard Authority of Ireland 2013). The concrete mix is C30/37 with a 0.55 water-to-cement ratio. Figure 3 shows details about the specimen design. The study designed the concrete specimen with three layers of reinforcements. The top and bottom layers provided the required tension, compression and flexure strength in the same manner as reinforced concrete slabs do. The middle layer, called the stopper layer, was used to control the crack growth so that the shape of the internal cracks could be as planar as possible. The depth of the middle layer can vary. As such, the study considered three possible locations: one at the middle of the specimen and the other two shifting up and down 4 cm relative to the middle line. The study fabricated three concrete specimens, with identical dimensions of 150 cm length by 80 cm width by 25 cm thickness.

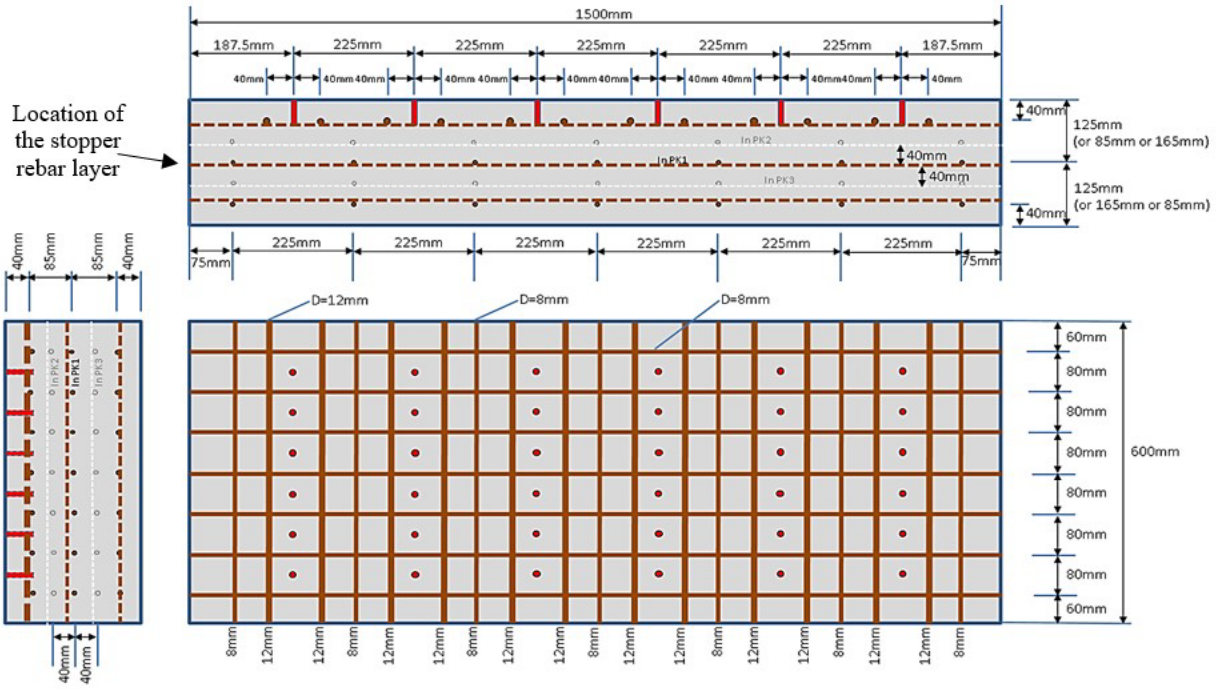

Source: FHWA.
InPK = three locations for the stopper layer.

Figure 3. Graph. Design dimensions for the concrete specimen.

Figure 4 shows a total of 36 polyvinyl chloride (PVC) cylinders, 8 mm in diameter and 5 cm in length, placed to create blind holes. The three concrete specimens were carefully fabricated in the laboratory (figure 5).

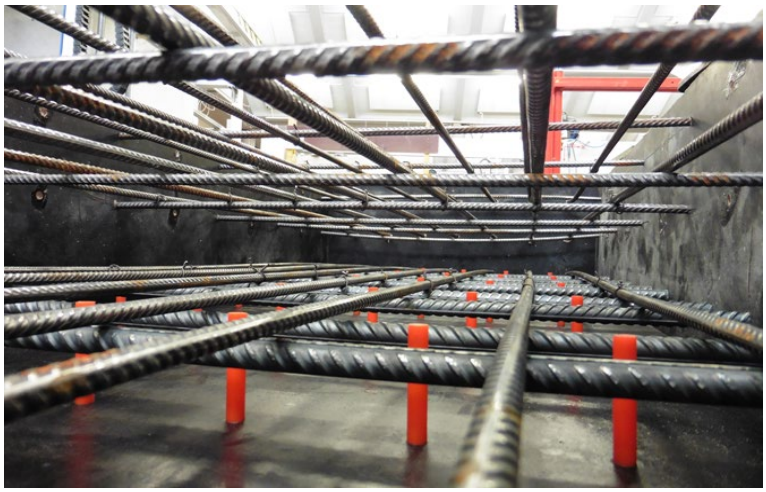

Source: FHWA.

Figure 4. Photo. Using PVC cylinders (red) to create boreholes in a concrete specimen, saving drilling effort.

Source: FHWA.

Figure 5. Photos. Specimen fabrication at Research Laboratory A.

The filling level of the expandable material should be 10 mm below the surface of the specimen to reduce the risk of breaking the concrete at the surface around the blind hole. It was not necessary to seal the exposed mortar at the top of the filling. Figure 6 shows that spalling occurred for holes filled to the surface of the concrete specimen. Figure 7 shows that filling the expandable material 10 mm below the surface level can prevent concrete spalling.

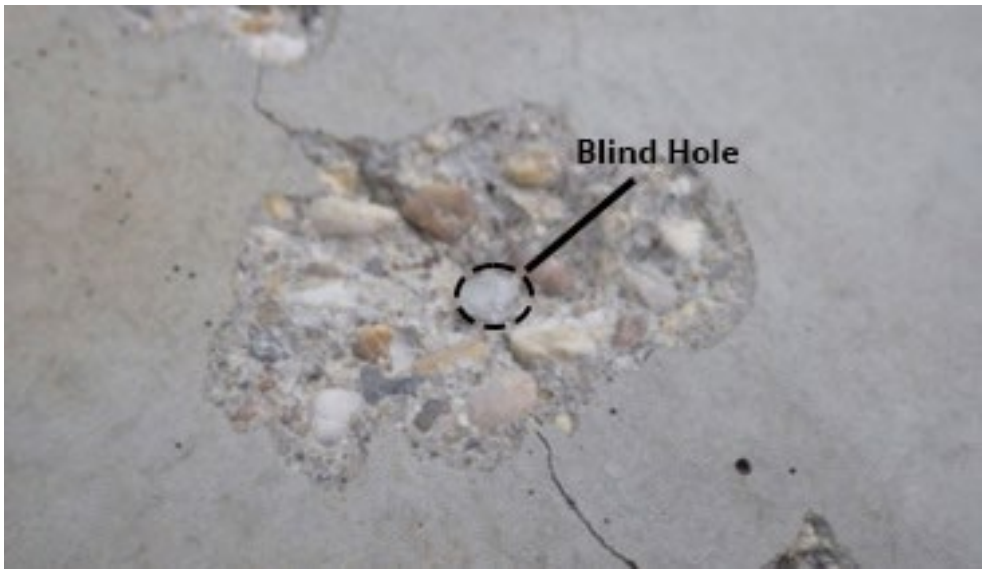

Source: FHWA.

Figure 6. Photo. Concrete spalling after expandable material was filled into the surface level.

Source: FHWA.

Figure 7. Photo. Cracks created without concrete spalling by filling expandable material in only to 10-cm below the surface level.

Figure 8 shows the plan views of the three specimens with cracks generated using the proposed method. The study used a crack gauge and macrophotographing to measure the width of surface cracks.

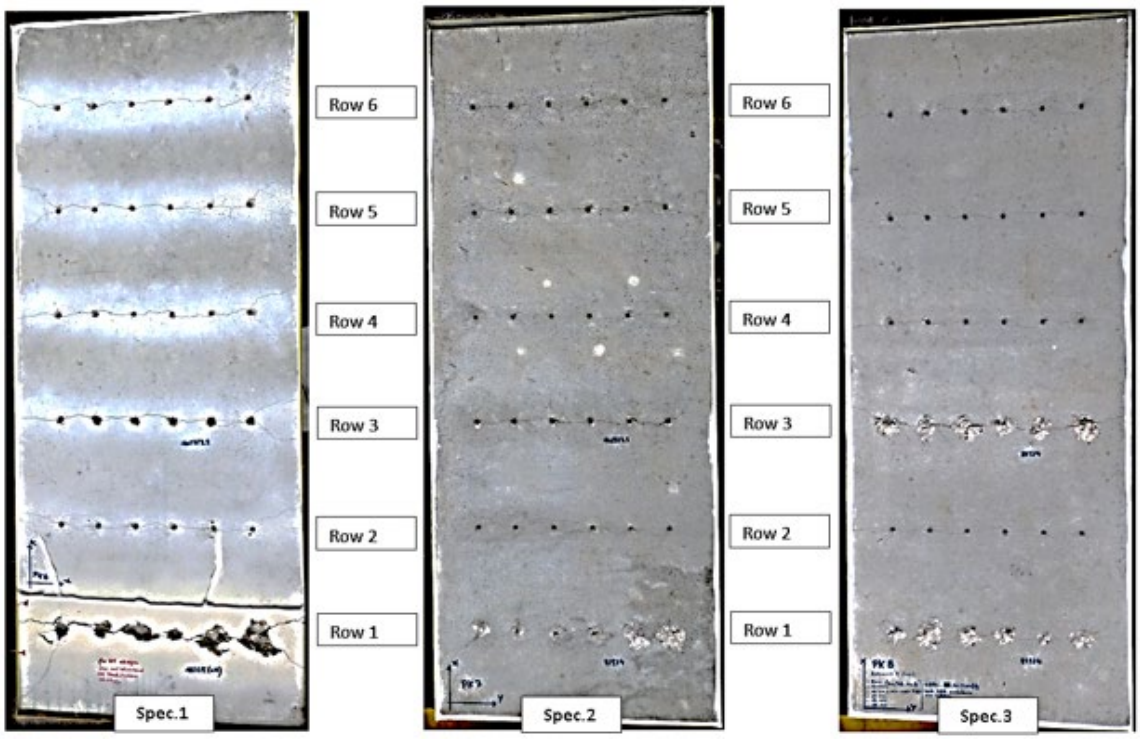

Source: FHWA.

Figure 8. Photos. Plan views of the three specimens after generation of desired cracks.

Source: FHWA.

Figure 9. Photos. Crack width measurement 3 d after filling the expandable material.

Figure 9 shows an example of the width measurement of surface cracks. The study evaluated the crack depth through destructive testing by cutting specimens perpendicular to a row of blind holes. The cutting process was carried out carefully in the lab (figure 10). Researchers applied the resin to guide the search for the internal cracks (figure 11).

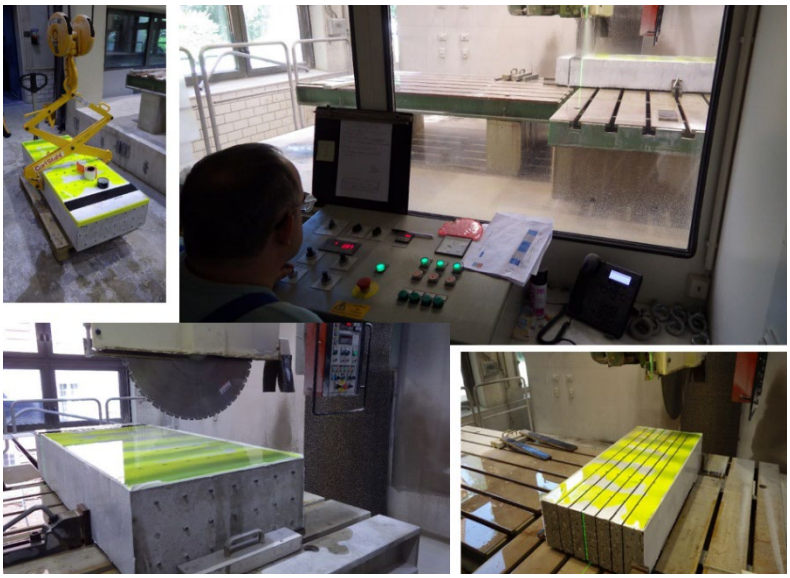

Source: FHWA.

Figure 10. Photos. Destructive testing to evaluate the internal cracks by cutting the specimen.

Source: FHWA.

Figure 11. Photos. Researchers apply resin to search for cracks.

Figure 12 shows the depth measurement of internal cracks on one side surface of a cut specimen. Depth measurements were performed on each side surface, with the naming conventions shown in figure 13.

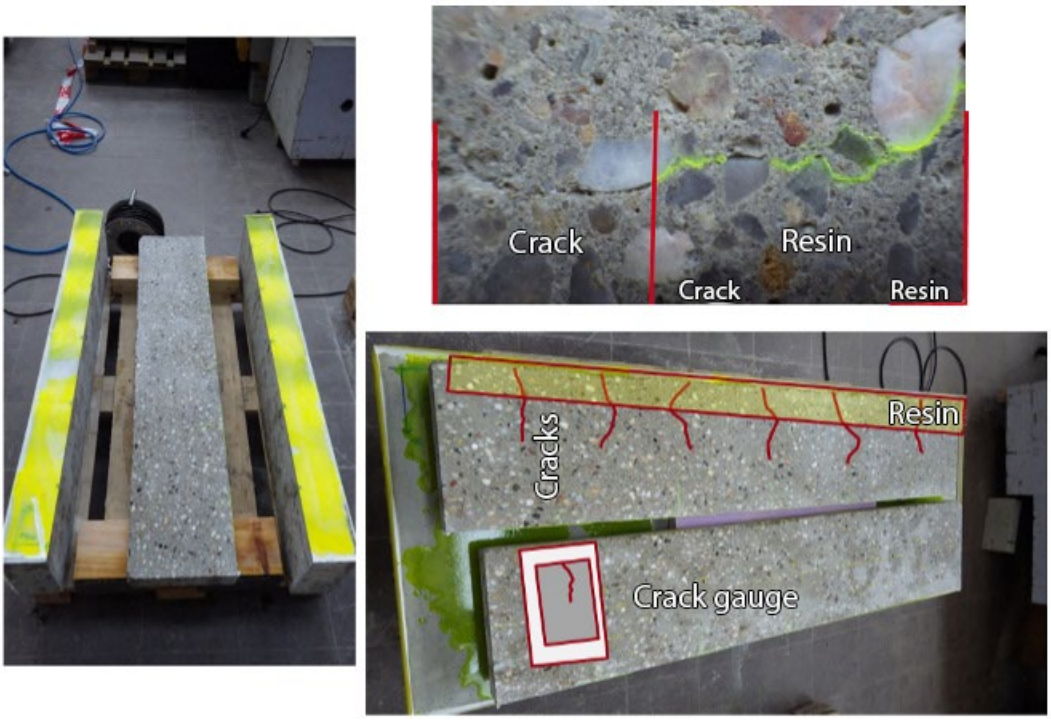

Source: FHWA.

Figure 12. Photos. Depth measurement of internal cracks.

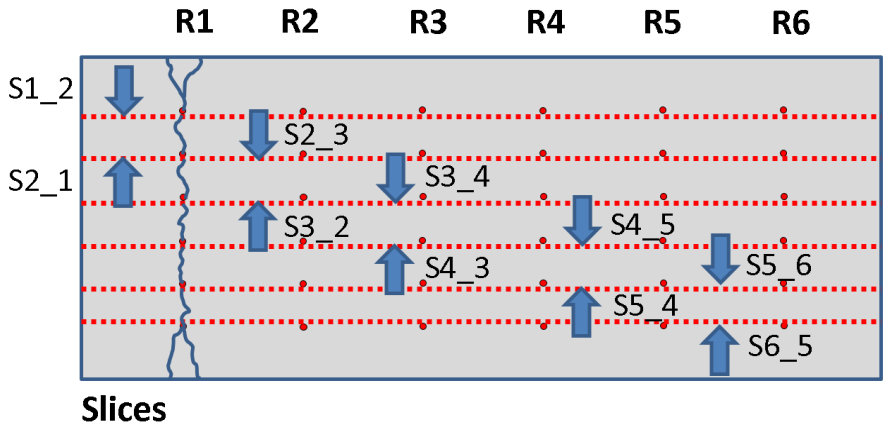

Source: FHWA.
S = slice; _ = side.

Figure 13. Graph. Naming convention for the crack depth measurement on two sides of a cut specimen.

Table 1 summarizes crack depth results. The standard deviation was in the range of aggregate sizes. The results confirmed that cracks could be reproduced following the procedures developed in this study.

Table 1. Crack depth measurement results.

Row No.	Side Surfaces										Mean	Standard deviation
	S1_2	S2_1	S2_3	S3_2	S3_4	S4_3	S4_5	S5_4	S5_6	S6_5		
R-1	12.50	12	11	14	15	11	13	13.5	15	12.5	12.95	1.44
R-2	15	13.5	13	13	13.5	11	13.5	13.5	13.5	14	13.35	1.00
R-3	17	13.5	12	14	15	16	15.5	15.5	15.5	16	15	1.45
R-4	13	14.5	12.5	12	15	14	13.5	12	16	14	13.65	1.31
R-5	14.5	14.5	14.5	12.5	14.5	13	17	14	17	12	14.35	1.67
R-6	12.5	10.5	12.5	17	13	12	13	14	14	12	13.05	1.72
Mean	13.75	13.25	13.13	13.63	14	12.5	14.25	13.38	15.13	13	13.6	1.43

Note: Values are in centimeters.
R = row; S = side.

VALIDATION BY RESEARCH LABORATORY B

Research Laboratory B developed a method by repeating the experiment using a local concrete mix with standard US reinforcement rebars #3 and #4. The #3 rebar had a diameter of 9.5 mm, and the #4 rebar had a diameter of 12.7 mm. These rebar dimensions were close enough to the dimensions in the original design to be compatible. The local concrete mix was specified with a compression strength of 4,000 psi.

The researchers found this developed method to be effective in generating the desired surface and internal cracks. Figure 14 shows that Research Laboratory B was able to use the developed method to generate surface cracks. Table 2 summarizes the depth measurements of internal cracks by Research Laboratory B. The results are similar to the crack depth measurements seen in table 1, confirming the effectiveness of the developed method.

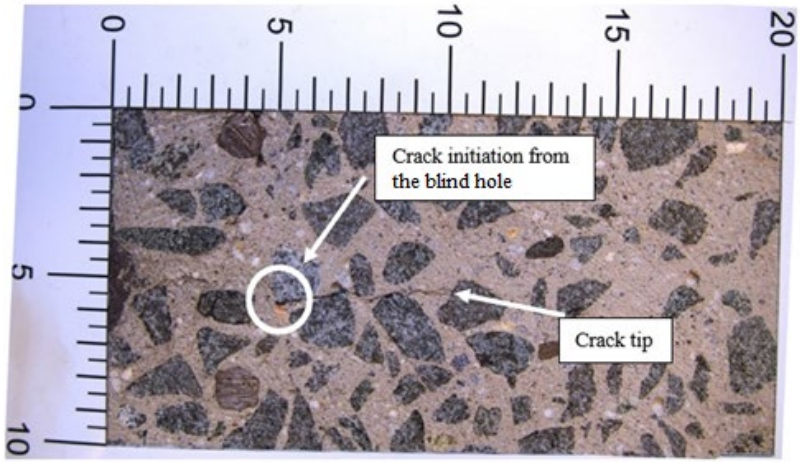

Source: FHWA.

Figure 14. Photo. Repeatable surface cracks generated by Research Laboratory B.

Table 2. Crack depth measurement results by Research Laboratory B.

Row No.	Side Surfaces										Mean	Standard deviation
	S1_2	S2_1	S2_3	S3_2	S3_4	S4_3	S4_5	S5_4	S5_6	S6_5		
R-1	11	9.5	8.5	8.5	11	11	9	11	13	11	10.3	1.43
R-2	12	12	9.5	11.5	11	11.5	11.5	8.5	12	10.5	11	1.17
R-3	10.5	9	9	10	9.5	7	9.5	11	10.5	11	9.7	1.2
R-4	8	8	15	13.5	16	12.5	12	18	12	17	13.2	3.43
R-5	15	17	8	11	11	13.5	11	14	12.5	17	13	2.87
R-6	8	8.5	10	14.5	12.5	13	12	13.5	11	15	11.8	2.39
Mean	10.75	10.7	10	11.5	11.8	11.4	10.8	12.7	11.8	13.5	11.5	2.08

Note: Values are in centimeters.

REMARKS

A method to generate surface and internal cracks was first studied by Research Laboratory A and then validated by Research Laboratory B. Although differences existed between concrete mixes and rebar dimensions, study results agreed with each other. The developed method can be a promising alternative to generate cracks in concrete reference specimens.

CHAPTER 4. DELAMINATION

BACKGROUND

Concrete delaminates from the structure when the corrosion-induced cracks in the concrete propagate, and the neighboring cracks join together to form a fracture plane that runs through the rebars (Li et al. 2007). Normally, concrete delamination represents a fracture plane formed under the structural surface. To artificially simulate the concrete delamination, a separation between concrete and reinforcements must be created. Inspired by the formation process of concrete delamination, this study developed a method to create this defect by injecting expandable material into the concrete specimen to generate crack propagation that formulates a fracture plane.

IMPLEMENTATION BY RESEARCH LABORATORY A

Figure 15 shows design details of the concrete specimen used in this study. The concrete mix was C30/37, as per European standard EN 206-1 (National Standard Authority of Ireland 2013). Researchers injected expandable material into the concrete specimen (see material details in Wiggenhauser et al. 2018). It took around 24 hr to generate cracks and formulate the delamination.

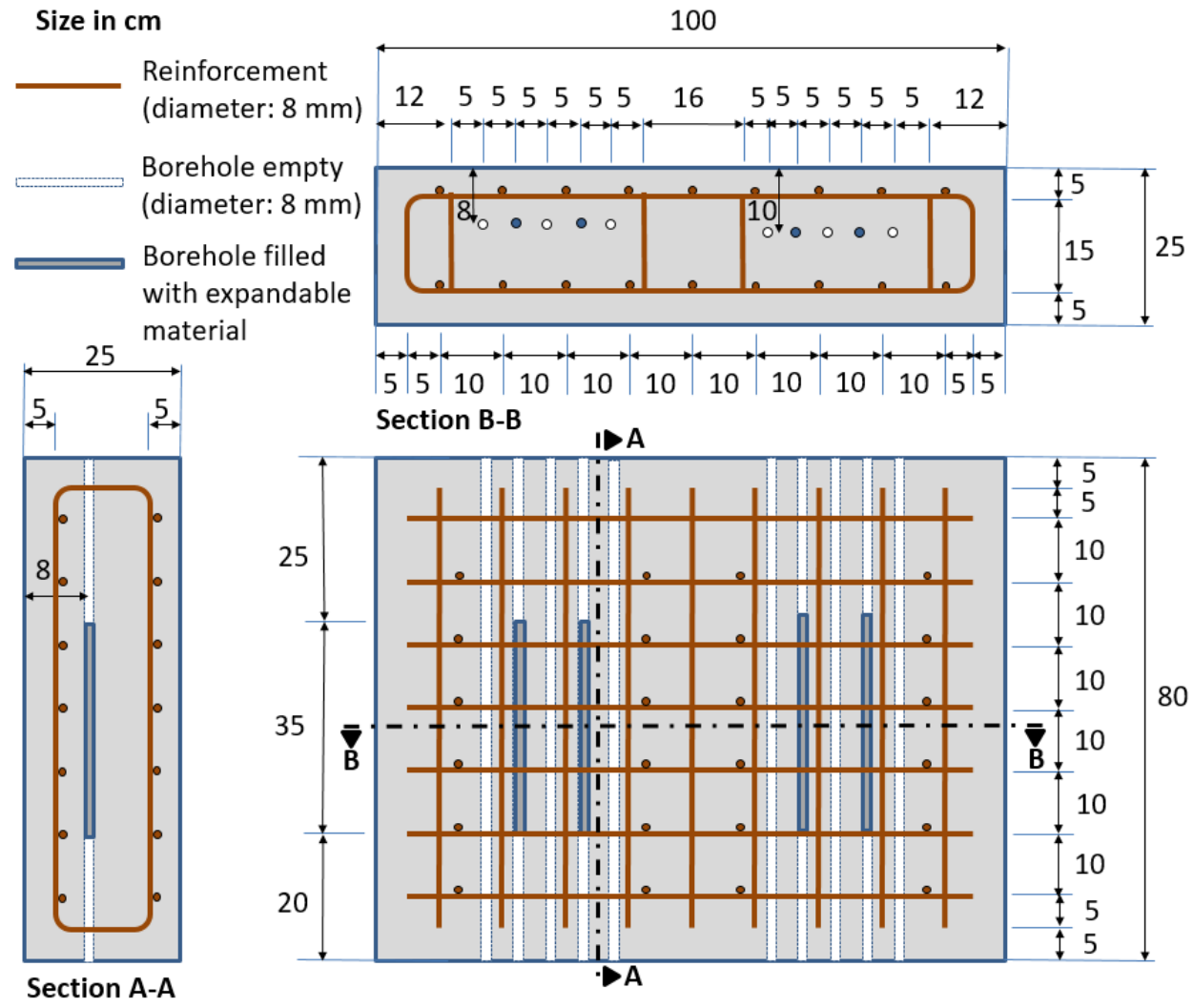

Source: FHWA.

Figure 15. Graph. Specimen design for creating concrete delamination.

Figure 16 shows the process of fabricating the specimen in the laboratory.

Source: FHWA.

Figure 16. Photo. Specimen fabrication.

Figure 17 shows a researcher injecting expandable material into a fabricated concrete specimen.

Source: FHWA.

Figure 17. Photo. Injecting expandable material into a concrete specimen.

Ultrasound tomography (UT) is a profound NDE approach to detect concrete delamination (Hoegh et al. 2011). UT testing utilizes an array of shear wave transducers to image potential defects in concrete structures. Analyzing the test results generally uses a visualization technique called the Synthetic Aperture Focusing Technique (SAFT) (Schickert et al. 2003). Despite the complexity of the SAFT technique, interpreting the results is straightforward; a strong reflection from a plane shallower than the thickness of the specimen indicates concrete delamination. This study used UT to detect the delamination created by the proposed method. Figure 18 shows the automated ultrasonic testing device. .

Source: FHWA.

Figure 18. Photo. Ultrasound tomographer used to detect delamination created in the specimen.

Figure 19 shows the UT test results on the concrete specimen. The results indicate the developed method successfully generated a fracture plane that effectively simulated the decimation.

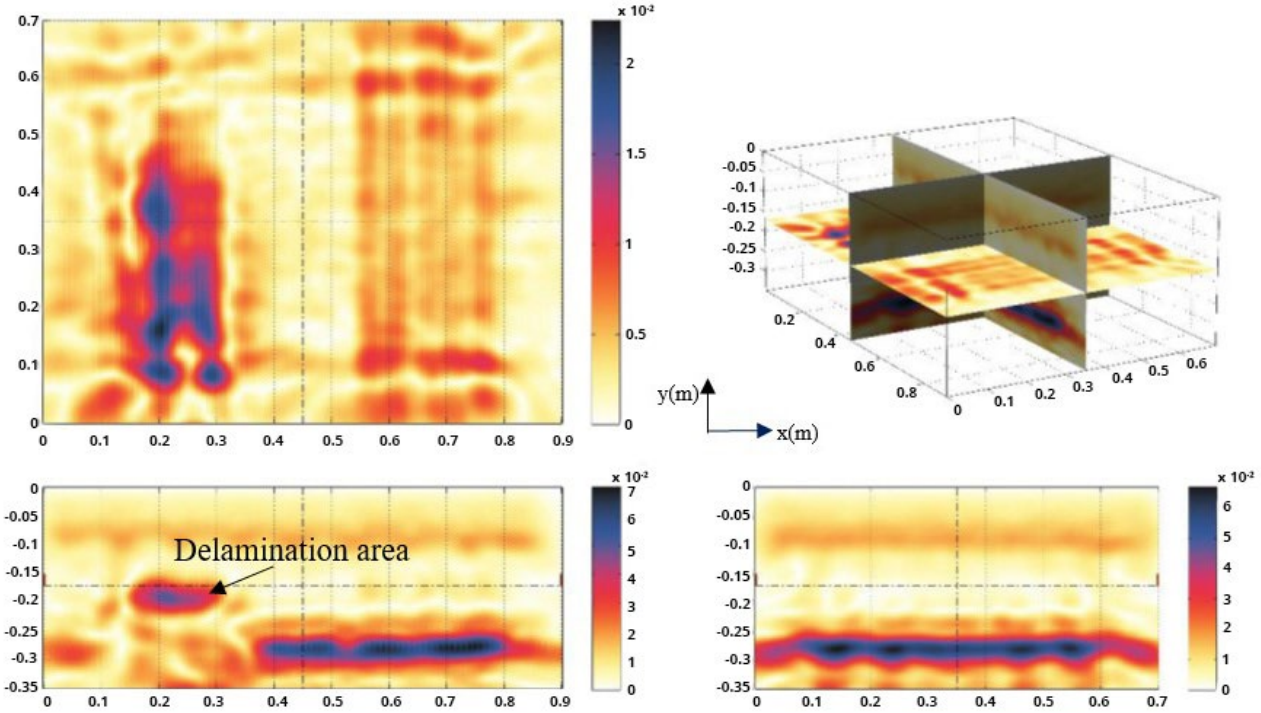

Source: FHWA.

Figure 19. Graph. UT test results showing delamination in the concrete specimen.

VALIDATION BY RESEARCH LABORATORY B

Research Laboratory B repeated the procedure developed by Research Laboratory A. The concrete mix was specified with a compression strength of 4,000 psi, as per American Concrete Institute (ACI) CODE-318-19(22): *Building Code Requirements for Structural Concrete and Commentary* (ACI 2022). The reinforcements were US #3 and #4 rebars, as per ASTM A615/A615M-20 *Standard Specification for Deformed and Plain Carbon-Steel Bars for Concrete Reinforcement* (ASTM 2022). The validation also used UT testing to evaluate the creation of delamination. The measuring grid was set to a size of 2 inches by 2 inches (figure 20).

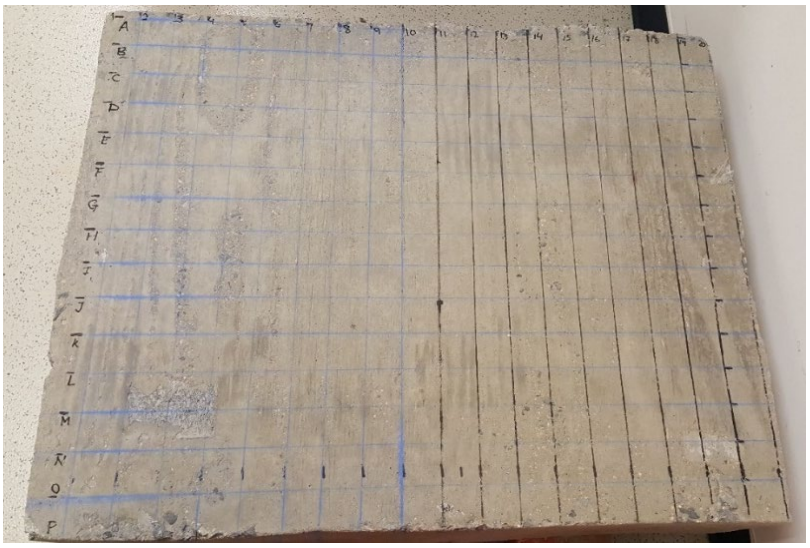

Source: FHWA.

Figure 20. Photo. Fabricated specimen at Research Laboratory B.

Figure 21 shows the UT test results, which indicate a delamination area was successfully created by the proposed method.

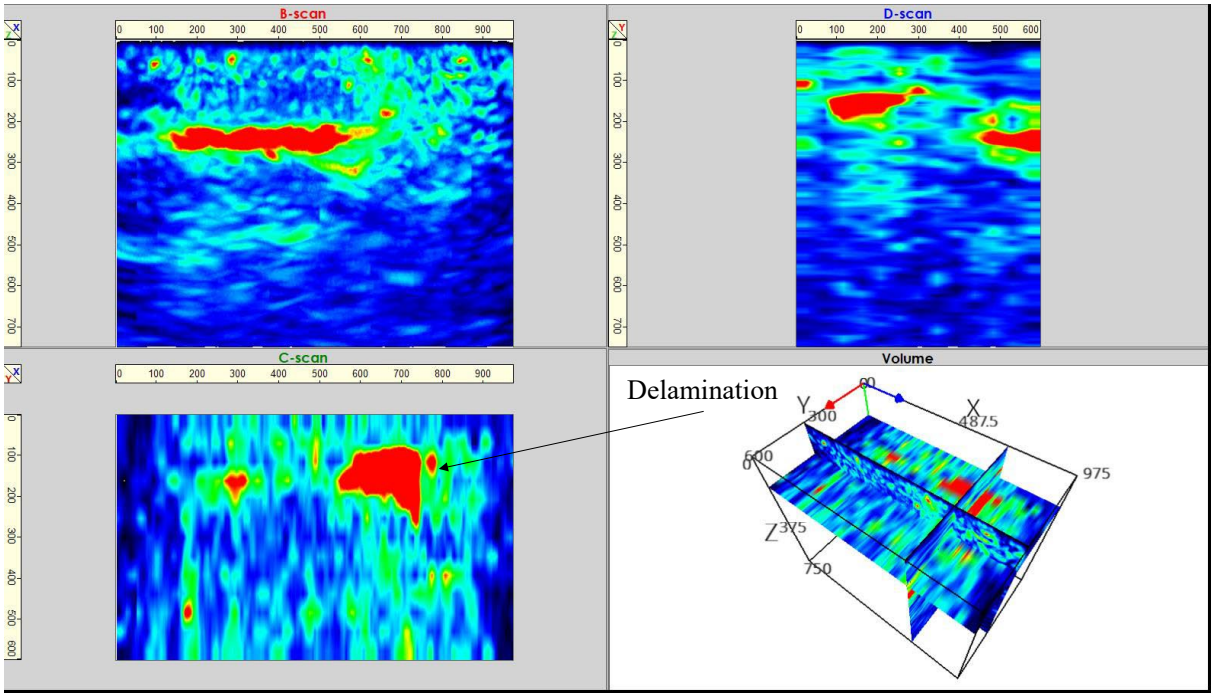

Source: FHWA.

Figure 21. Graph. UT test results showing created delamination in the concrete specimen fabricated at Research Laboratory B.

REMARKS

The study developed a method to artificially create delamination areas by injecting expandable material into fabricated concrete specimens. The procedure was first developed by Research Laboratory A and then validated by Research Laboratory B. The study used UT as a nondestructive approach to identify the delamination generated by the developed method. The study results suggest this approach was able to generate a fracture plane shallower than the thickness of the concrete specimen. This method is promising for artificially simulating concrete delamination without injecting external nonconcrete objects.

CHAPTER 5. HONEYCOMBING

BACKGROUND

Honeycombing in concrete is a structural deficiency stemming from suboptimal compaction during construction, visually similar to honeybee nests. Honeycombing is an undesirable phenomenon because it can reduce the concrete's compressive strength and durability. The attribution factors of honeycombing may include improper vibration techniques, inadequacies in the concrete mix composition, and deficiencies in formwork installation. Honeycombing is usually artificially created by inserting intentionally reduced compacted concrete blocks or honeycombs into the concrete slab.

This study aims to validate this method with local concrete mixes and reinforcements. As described in chapter 3, UT can be an effective NDE tool to detect hollow concrete defects. This study uses UT to evaluate the effectiveness of the fabrication method for creating concrete specimens with honeycombs.

IMPLEMENTATION BY RESEARCH LABORATORY A

Figure 22 shows the specimen design used in this study. The concrete mix was C30/37 (EN 206-1) with a water-to-cement ratio of 0.55 ((National Standard Authority of Ireland 2013). The specimen consisted of honeycombs with various locations and orientations.

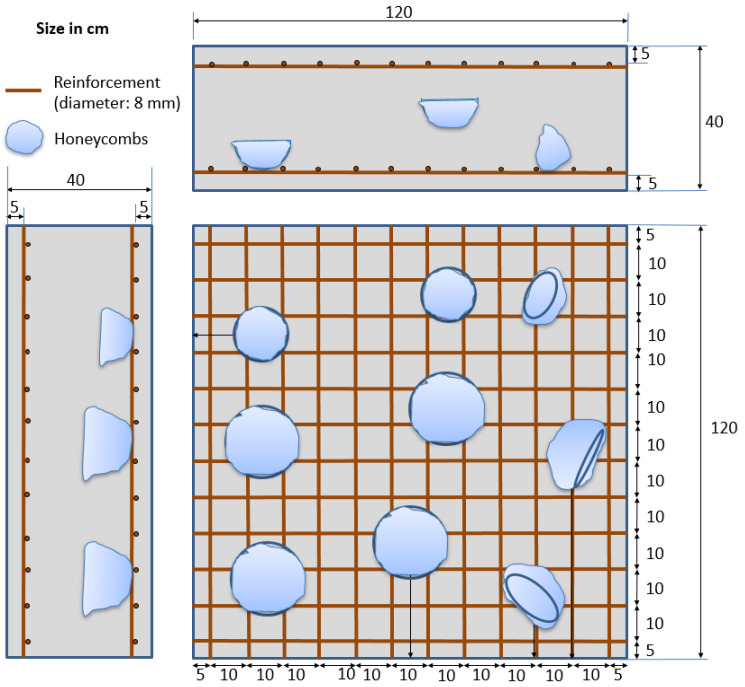

Source: FHWA.

Figure 22. Graph. Specimen design with honeycombs.

Figure 23 shows the prefabricated honeycombs used in this study. The research team individually fabricated the honeycombs by mixing aggregates, cement, and water in various sizes. Suboptimal mixing ratios were deliberately used to create honeycombing elements that yielded lower densities than surrounding material.

Source: FHWA.

Figure 23. Photo. Prefabricated honeycombs in different sizes.

Figure 24 shows the fabrication process.

Source: FHWA.

Figure 24. Photo. Specimen fabrication with preinserted honeycombs.

Figure 25 shows the UT test results detecting the preinserted honeycombs. Researchers identified honeycombing regions by noting the appearance of strong reflections at shallower depths than specimen thickness.

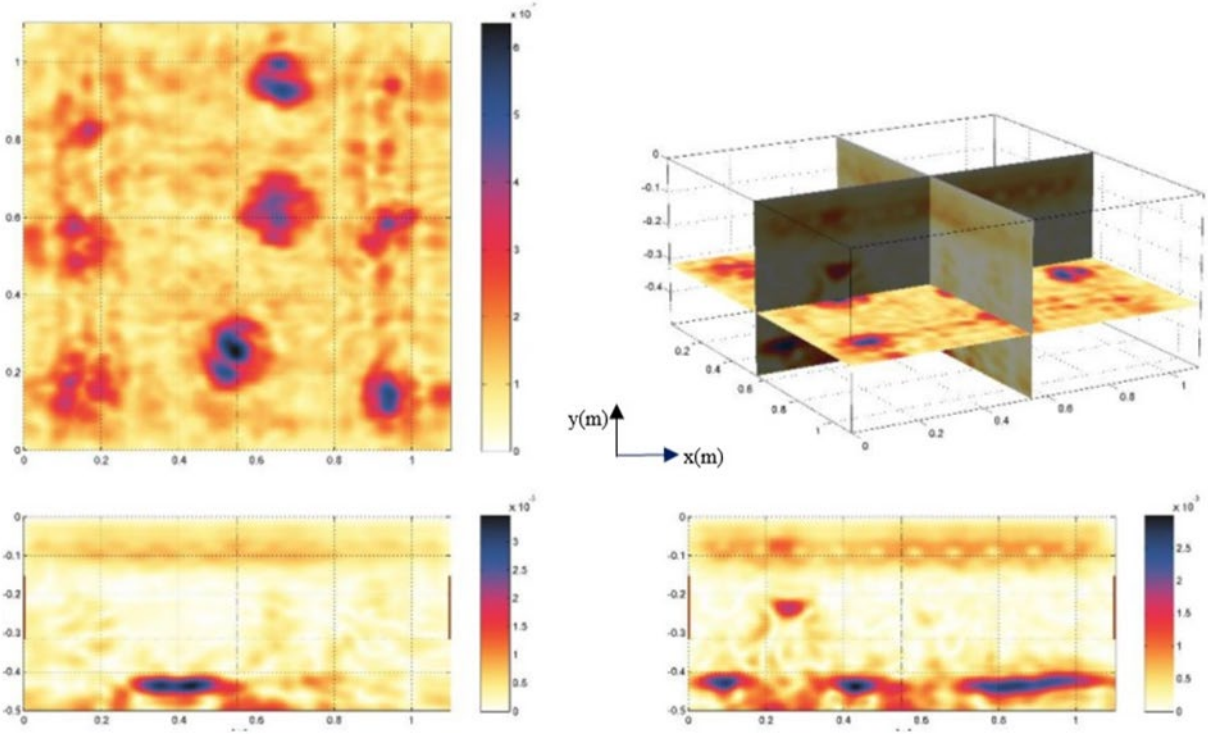

Source: FHWA.

Figure 25. Graph. UT test results to detect preinserted honeycombs.

VALIDATION BY RESEARCH LABORATORY B

Research Laboratory B repeated the process by using local concrete mixes and US standard #3 rebars. The concrete mix was specified with a compressive strength of 4,000 psi. Figure 26 shows that multiple honeycombs were placed in various locations of the specimen before the concrete was poured.

Source: FHWA.

Figure 26. Photo. Specimen with preinserted honeycombs by Research Laboratory B.

Figure 27 shows the fabricated specimen after the concrete was poured.

Source: FHWA.

Figure 27. Photo. Fabricated specimen with preinserted honeycombs.

Figure 28 shows the UT test results to detect the preinserted honeycombs. Researchers identified honeycombing regions by noting the appearance of strong reflections at shallower depths than specimen thickness.

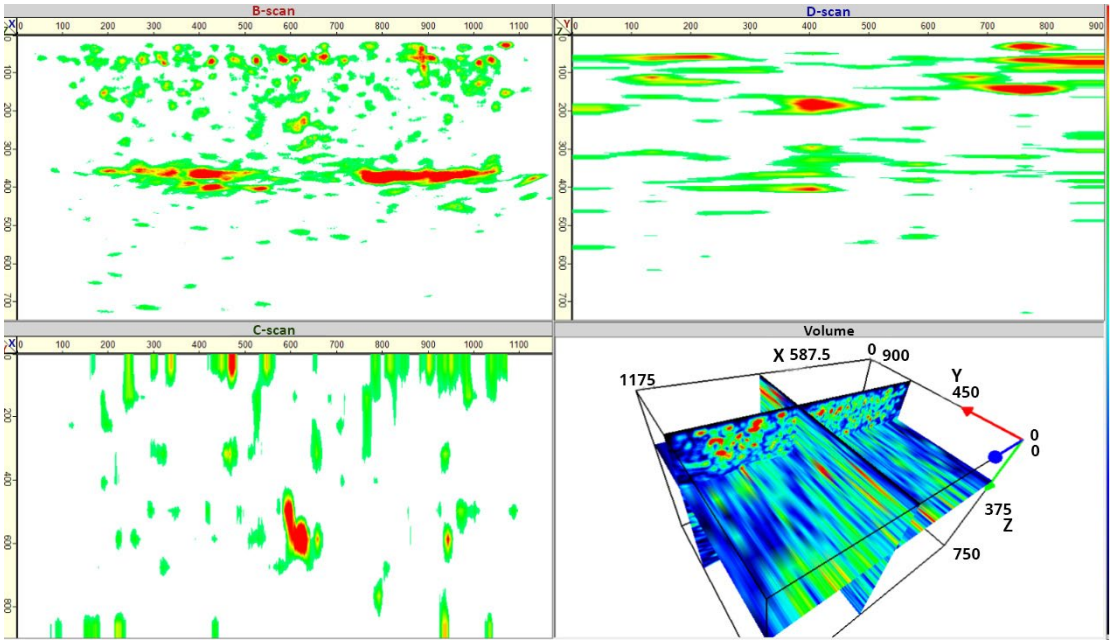

Source: FHWA.

Figure 28. Graph. UT test results to detect preinserted honeycombs.

REMARKS

This study validated an approach for creating concrete specimens with artificial honeycombs using local concrete mixes and reinforcements. The approach involves inserting prefabricated honeycombs before pouring concrete. The study results show that this approach is effective, indicated by successful detections of honeycombs using UT. Researchers identified honeycombing regions by noting the appearance of strong reflections at depths shallower than specimen thickness.

CHAPTER 6. REINFORCEMENT CORROSION

BACKGROUND

This study applied electric current to generate reinforcement corrosion in concrete specimens. Figure 29 illustrates the principle of applying electric current in a concrete specimen with two rods: one serves as the anode, the other as the cathode. The electric current can generate corrosion and cause material losses after brushing off the corroded part. Thus, measuring material losses can be an effective method to evaluate the corrosion induced by the electric current. However, measuring material losses requires destructive evaluation of the concrete specimen.

An alternative approach is to use ground-penetrating radar (GPR) as a nondestructive method. ASTM D6087, *Standard Test Method for Evaluating Asphalt-Covered Concrete Bridge Decks Using Ground Penetrating Radar,* provides a standard test that uses GPR to detect corrosion in concrete bridge decks (ASTM 2022). Corrosion is indicated in rebars by lower reflection amplitudes from corroded rebars than from intact rebars. The visualization of the reflection amplitude of GPR signals, or the B-scan, is normally plotted in grayscale, with a larger amplitude toward the lightest areas and a lower amplitude toward the darkest.

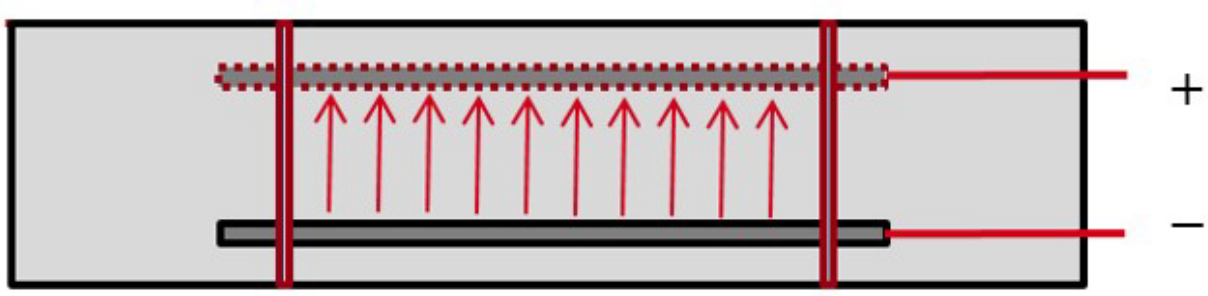

Source: FHWA.

Figure 29. Graph. Applying electric current to generate corrosion in a concrete specimen.

IMPLEMENTATION BY RESEARCH LABORATORY A

Figure 30 shows the concrete specimen used in this study. The specimen consisted of four pairs of metal rods with different lengths (12 cm, 17 cm, 22 cm, and 42 cm). Applying the same ampere of electric current to metal rods with different lengths can generate different levels of corrosion. Shorter metal rods were expected to have higher levels of corrosion. Cables were connected to the metal rods and secured to prevent any short-circuit currents. A constant current of 10 mA was applied to the circuit.

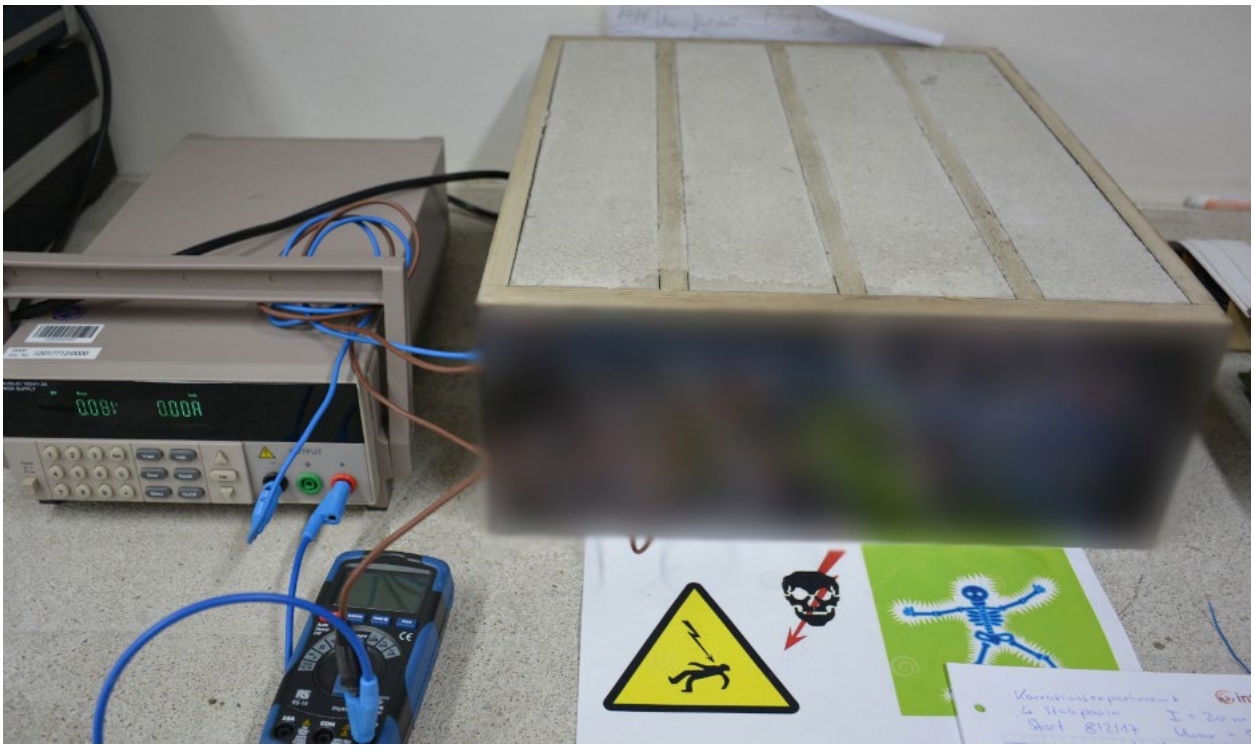

Source: FHWA.

Figure 30. Photo. Wired specimen is investigated for effects of rebar length by applying the same ampere and period of electric current.

Figure 31 shows the voltage and current applied during the test. When the maximum voltage of 150 V was reached, the experiment was stopped for safety reasons.

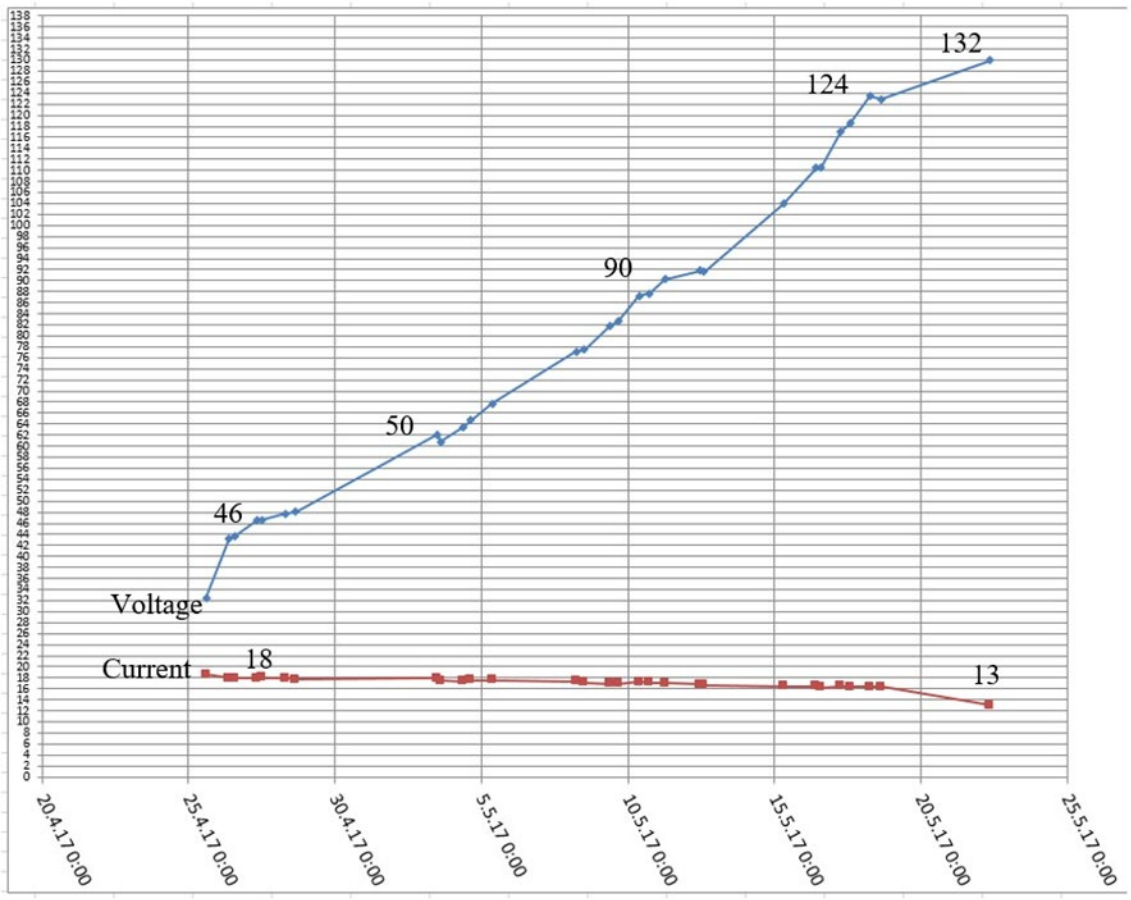

Source: FHWA.

Figure 31. Graph. Specimen fabrication.

Material loss was measured by destructive evaluations. Table 3 shows the weight loss of the four rods. Figure 32 shows one of the rods in each pair (the negative conductor) remained intact as the other (the positive conductor) corroded. The metal rods were removed from the concrete carefully. Corrosion products were removed with a brush. The material loss was measured by comparing the original weight of the rods to the weight after the corrosion products were brushed off.

Table 3. Weight measurements to evaluate corrosion-induced weight loss.

Rod Number	Before (g)	After (g)	Difference/ Absolute Change (g)	Relative Weight Reduction (Percent)	Length (cm)	Corrosion Per Length (g/cm)
1	45.44	41.82	3.63	7.98	12	0.302
3	62.76	61.81	0.95	1.51	17	0.056
5	84.49	83.78	0.71	0.85	22	0.032
7	163.24	162.70	0.54	0.33	42	0.013

Source: FHWA.

Figure 32. Photo. Destructive evaluation of concrete specimens to measure material loss.

VALIDATION BY RESEARCH LABORATORY B

Research Laboratory B repeated the procedure developed by Research Laboratory A by using local concrete mixes and US standard rebars. Possibly due to the use of different concrete mixes, researchers found minimal corrosion at the beginning of the test. In order to accelerate the corrosion process, Research Laboratory B applied a solution of 3.5-percent magnesium chloride anhydrous, 99-percent by weight in a basin on top of the concrete surface. Figure 33 shows the fabricated specimen used in this study. Visual inspection of figure 33 indicates corrosion was generated around all rebars, and a higher level of corrosion was generated in the right pairs of rebars than in the left and middle pairs.

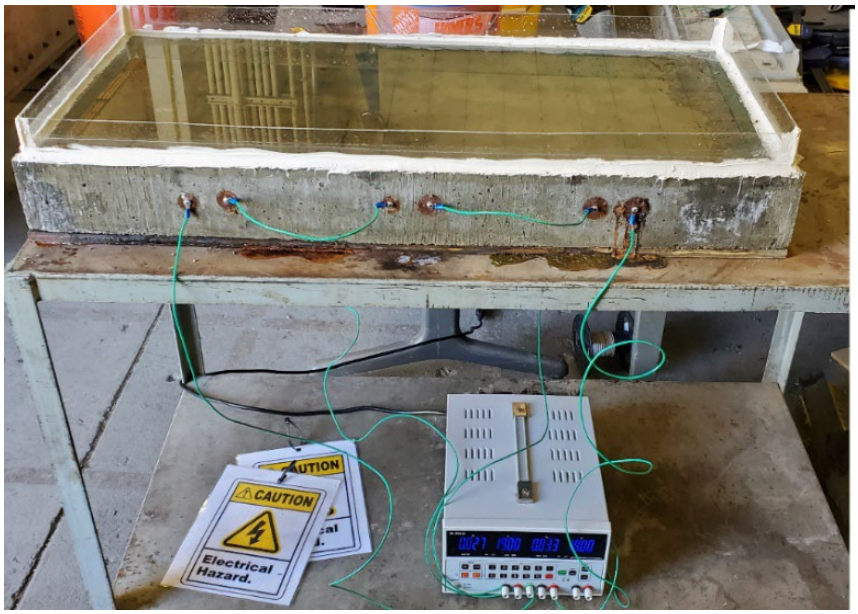

Source: FHWA.

Figure 33. Photo. Concrete specimen fabricated by Research Laboratory B to generate corrosion.

The corrosion of the steel rods was assessed using GPR. A GPR system equipped with a 1.6-GHz antenna was used. Figure 34 shows GPR B-scans in a longitudinal direction on top of each pair of rebars; the reflection amplitude of GPR signals was lower on the right pairs of rebars than on the left and middle pairs. Results confirmed that a higher level of corrosion was generated on the right pairs of rebars compared to the left and the middle pairs.

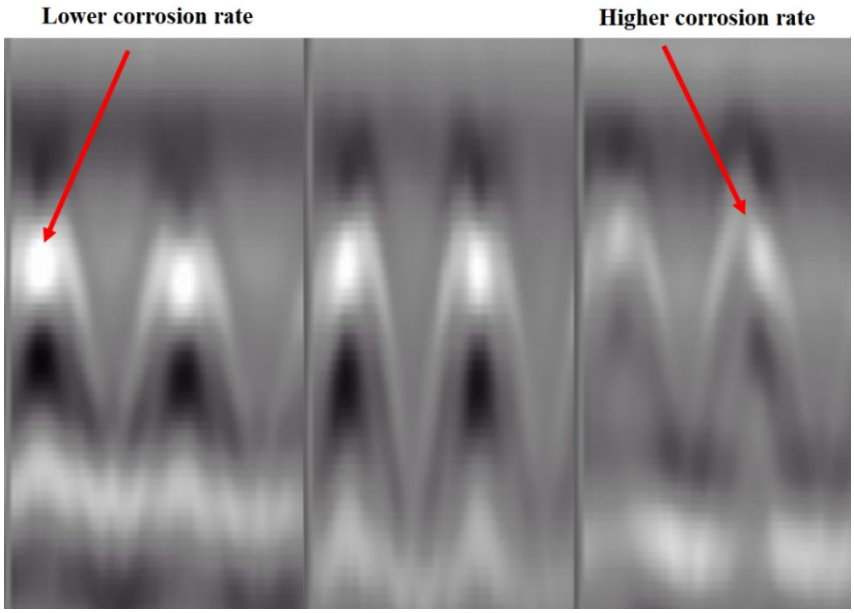

Source: FHWA.

Figure 34. Graph. GPR B-scans show a higher level of corrosion on the right pairs of steel rebars.

REMARKS

The study developed and validated a method to artificially generate corrosion in concrete specimens. The method involves applying electric current to reinforcing rebars in the specimen. The study found that applying the same ampere and period of electric current to rebars with different lengths generated different levels of corrosion. Destructive evaluation of the corrosion indicates rebar with a shorter length will receive a higher level of corrosion, indicated by a larger material or weight loss. The effectiveness of applying electric current may vary due to different concrete mixes. Corrosion can be accelerated by fabricating a basin containing saltwater solution on top of the concrete surface.

CHAPTER 7. SUMMARY

This report documented a series of experiments that sought to fabricate concrete specimens that contained artificial defects, including cracks, delamination, honeycombing, and reinforcement corrosion. These defects are common structural defects observed in concrete structures. The findings presented in this report can benefit future research by providing the means to generate fabricated specimens with known types of defects at known locations. Fabricated specimens can serve as good resources for research, training and education, and certification programs.

After a literature review of related studies (as discussed in more detail in chapter 2), the research team developed innovative approaches to generating concrete cracks and delamination. The current practice in fabricating reference specimens involves embedding extraneous objects (like foils or plastic sheets) in specimens, which is a practice that may later influence test results and interpretations. The proposed approach in this study involves injecting expandable material into concrete specimens, creating internal forces, and generating cracks. This approach is beneficial in that it does not insert nonconcrete objects and thus mitigates the effect of the object's properties to some extent. The study demonstrated and validated this approach. Destructive and NDE tests demonstrated that the study successfully created cracks and delamination in fabricated concrete specimens.

Additionally, the study validated a common approach to simulate honeycombs in concrete using local concrete mixes and reinforcements. The study results confirmed the effectiveness of the approach in fabricating specimens with honeycombing.

The study also validated a common approach for generating corrosion in concrete rebars by applying electric currents. The study confirmed the effectiveness of applying electric currents.

Additionally, the study found that the amount of corrosion generated varied with rebars length. Under the same ampere of electric current for the same period, a shorter rebar presented a higher level of corrosion. A higher level of corrosion represented a larger loss of material, in terms of rebar weight. However, the effectiveness of methods can vary due to different concrete mixes. Using a basin containing saltwater can accelerate the corrosion process.

REFERENCES

ACI. 2022. ACI CODE-318-19(22): *Building Code Requirements for Structural Concrete and Commentary*. Farmington Hills, MI: American Concrete Institute.

ASTM. 2022. ASTM D6087-22 *Standard Test Method for Evaluating Asphalt-Covered Concrete Bridge Decks Using Ground Penetrating Radar*. West Conshohocken, PA: ASTM International.

ASTM. 2022. ASTM A615/A615M-20 *Standard Specification for Deformed and Plain Carbon-Steel Bars for Concrete Reinforcement*. West Conshohocken, PA: ASTM International.

Bogas, J. A., H. H. Ahmed, and T. Diniz. 2021. "Influence of Cracking on the Durability of Reinforced Concrete With Carbon Nanotubes." *Applied Sciences* 11, 4: 1–18. https://doi.org/10.3390/app11041672, last accessed October 18, 2023.

Hasan, M. I., and N. Yazdani. 2016. "An Experimental Study for Quantitative Estimation of Rebar Corrosion in Concrete Using Ground Penetrating Radar." *Journal of Engineering* 2016. https://doi.org/10.1155/2016/8536850, last accessed October 18, 2023.

Hoegh, K., L. Khazanovich, and H. T. Yu. 2011. "Ultrasonic Tomography for Evaluation of Concrete Pavements." *Transportation Research Record* 2232: 85–94. https://doi.org/10.3141/2232-09, last accessed October 18, 2023.

Kee, S. H., and N. Gucunski. 2016. "Interpretation of Flexural Vibration Modes From Impact-Echo Testing." *Journal of Infrastructure Systems* 22, 3. https://doi.org/10.1061/(asce)is.1943-555x.0000291, last accessed October 18, 2023.

Li, C. Q., J. J. Zheng, W. Lawanwisut, and R.E. Melchers. 2007. "Concrete Delamination Caused by Steel Reinforcement Corrosion." *Journal of Materials in Civil Engineering* 19, 7: 591–600. https://doi.org/10.1061/(asce)0899-1561(2007)19:7(591), last accessed October 18, 2023.

Lin, S., D. Meng, H. Choi, S. Shams, and H. Azari. 2018. "Laboratory Assessment of Nine Methods for Nondestructive Evaluation of Concrete Bridge Decks With Overlays." *Construction and Building Materials* 188: 966–982. https://doi.org/10.1016/j.conbuildmat.2018.08.127, last accessed October 18, 2023.

National Standard Authority of Ireland. 2013. EN 206-1:2000/A2:2005*—Concrete—Part 1: Specification Performance, Production and Conformity.* Haymarket, Australia: SAI Global.

Oh, T., J. S. Popovics, and S. H. Sim. 2013. "Analysis of Vibration for Regions Above Rectangular Delamination Defects in Solids." *Journal of Sound and Vibration* 332, 7: 1766–1776. https://doi.org/10.1016/j.jsv.2012.11.003, last accessed October 18, 2023.

Sansalone, M., and N. J. Carino. 1989. "Detecting Delaminations in Concrete Slabs With and Without Overlays Using the Impact-Echo Method." *ACI Materials Journal* 86, 2: 175–184. https://doi.org/10.14359/2350, last accessed October 18, 2023.

Schickert, M., M. Krause, and W. Müller. 2003. "Ultrasonic Imaging of Concrete Elements Using Reconstruction by Synthetic Aperture Focusing Technique." *Journal of Materials in Civil Engineering* 15, 3: 235–246. https://doi.org/10.1061/(asce)0899-1561(2003)15:3(235), last accessed October 18, 2023.

Stefan, M., V. Salvador, and S. David. 2018. "Validation of Artificial Defects for Non-Destructive Testing Measurements on a Reference Structure." *MATEC Web of Conferences* 199. https://doi.org/10.1051/matecconf/201819906006, last accessed October 18, 2023.

Torkornoo, S., E. Bradshaw, S. R. Sharp, and M. M. Sprinkel. 2018. *Design of Artificially Cracked Concrete Specimens for Virginia Department of Transportation Material Evaluation*. Report No. VTRC [Virginia Transportation Research Council] 18-R2. https://www.virginiadot.org/vtrc/main/online_reports/pdf/18-r2.pdf, last accessed October 18, 2023.

Tran, Q., and J. R. Roesler. 2022. "Rapid Detection of Concrete Joint Activation Using Normalized Shear Wave Transmission Energy." *International Journal of Pavement Engineering* 23, 4: 1025–1037. https://doi.org/10.1080/10298436.2020.1785448, last accessed October 18, 2023.

Wiggenhauser, H., C. Köpp, J. Timofeev, and H. Azari. 2018. "Controlled Creating of Cracks in Concrete for Non-Destructive Testing." *Journal of Nondestructive Evaluation* 37, 3. https://doi.org/10.1007/s10921-018-0517-x, last accessed October 18, 2023.

Zhang, H., L. Liao, R. Zhao, J. Zhou, M. Yang, and R. Xia. 2016. "The Non-Destructive Test of Steel Corrosion in Reinforced Concrete Bridges Using a Micro-Magnetic Sensor." *Sensors* 16, 9. https://doi.org/10.3390/s16091439, last accessed October 18, 2023.

Zhu, J., and J. S. Popovics. 2007. "Imaging Concrete Structures Using Air-Coupled Impact-Echo." *Journal of Engineering Mechanics* 133, 6: 628–640. https://doi.org/10.1061/(asce)0733-9399(2007)133:6(628), last accessed October 18, 2023.

Recommended citation: Federal Highway Administration,
Development of Reference Specimens for Laboratory Testing
(Washington, DC: 2024) https://doi.org/10.21949/1521373

HRDI-20/05-24(WEB)E